CHAPTER 3

RESULTS AND DISCUSSION

The research included the development and verification of the earlier apparatus, and the collection and validation of moisture diffusion data under both isothermal and nonisothermal conditions. The main objective of the apparatus is to measure the moisture (water vapor) flux rate through a given hygroscopic material under various conditions. The test material for which data was obtained during the experimental procedure of this research is oriented strand board (OSB), which is a wood composite material. The test specimen consists of a disk of 0.4318 m (17 in.) in diameter and 6.4 mm (0.25 in.) in thickness.

The performance of the controls systems of the apparatus as well as the data obtained are presented in this chapter. The first section covers the operation of both the instrumentation and the control systems. The results obtained both during isothermal and nonisothermal tests are presented in the second section. The data validation, results and discussion of additional experiments are presented in the last section of this chapter.

3.1 APPARATUS OPERATION

The validation of the apparatus results relies on the accuracy of the temperature and the relative humidity maintained within the chambers. The validity of the data collected depends upon the accuracy in the control of the temperature and relative humidity. On the other hand, the control stability depends on the accuracy of the instruments and the reliability of the controllers.

The high end range of the relative humidity within the apparatus is limited by the lowest temperature encountered within the apparatus, since this temperature will dictate the dew point of the system. At temperatures of 0^oC to 5^oC, the maximum relative humidity allowed is approximately 68 per cent as a direct result of the low dew-point temperatures. At operating temperatures around room temperature the maximum allowable relative humidity is approximately 75 per cent. The temperature control system of the apparatus is capable of maintaining a temperature difference of 10^oC across the specimen with a maximum variation of $\pm 0.05^oC$.

3.1.1 Instrumentation

As indicated in the previous chapter, it is extremely important to maintain close control of the temperature and relative humidity within the chambers. This section focuses on the accuracy of the instruments used to control the environmental conditions of the apparatus.

The control system uses an instrument manufactured by Vaisala which measures temperature and relative humidity. The Vaisala transmitter was calibrated directly at the factory at the time of purchase. This calibration indicated an uncertainty of ±0.6 per cent R.H. and $\pm 0.2^oC$. The calibration and instrument verification as indicated by the manufacturer used dry nitrogen and a set of controlled aqueous salt solutions. The temperature calibration of the Vaisala instrument was performed at ambient temperature (25°C) against a Fluke 8520A/PRT.

A separate calibration check was performed with the instrument assembled inside the chamber. A dew-point hygrometer (General Eastern) and a Fluke temperature transducer verified the relative humidity and temperature, respectively. The dew-point hygrometer used for the calibration of the instrument uses optical hygrometry principles. Optical hygrometry is a precise technique, which determines the water vapor content in gases by measuring dew- or frost-point temperatures. Optical condensation hygrometry is based on the chilled-mirror principle. The surface of the chilled-mirror is cooled until it reaches a temperature at which condensation begins to form on it, at this point an

optical sensor detects the condensation and its temperature is measured. The measured temperature corresponds to the dew point.

The dew-point temperature within each chamber was calculated taking into account the actual pressure in the chamber, and compared to the read out corresponding to the hygrometers. The difference between the measured and calculated dew point temperatures (0.5^{o}C) were within the accuracy of both instruments, ±0.6 per cent R.H. for the Vaisala and ±0.2^{o}C for the hygrometer.

The temperature indicated by the Vaisala instrument was compared to a Fluke temperature transducer using a type-*T* thermocouple. Once again the difference between the measured temperatures (±0.1^{o}C) were within the uncertainty of both instruments.

Calibration was performed on each Vaisala instrument at different levels of relative humidity while running an isothermal test at 25°C.

3.1.2 Temperature Control

As discussed in the previous chapter, the environmental controls are a critical and essential part of the proper operation of the apparatus. The control stability allows the system to reach and sustain steady state conditions faster. The temperature control system was designed to maintain strong nonisothermal conditions across the sample material. In general, the nonisothermal tests were conducted under two different temperature differences, 5 and 10 degrees Celsius, corresponding to a temperature gradient of 7.87 and 15.74 °C/cm, respectively. Figure 3.1 shows the temperature of each chamber over a period of 12 days. The accuracy and performance of the temperature control system can be observed in the enlarged plots depicted in Fig. 3.2.

Even with 10°C temperature differences, the control maintained the temperature inside each chamber within ±0.1^{o}C of the set point. The plots seen in Fig. 3.1-2 were generated by data obtained by the computer every 10 minutes.

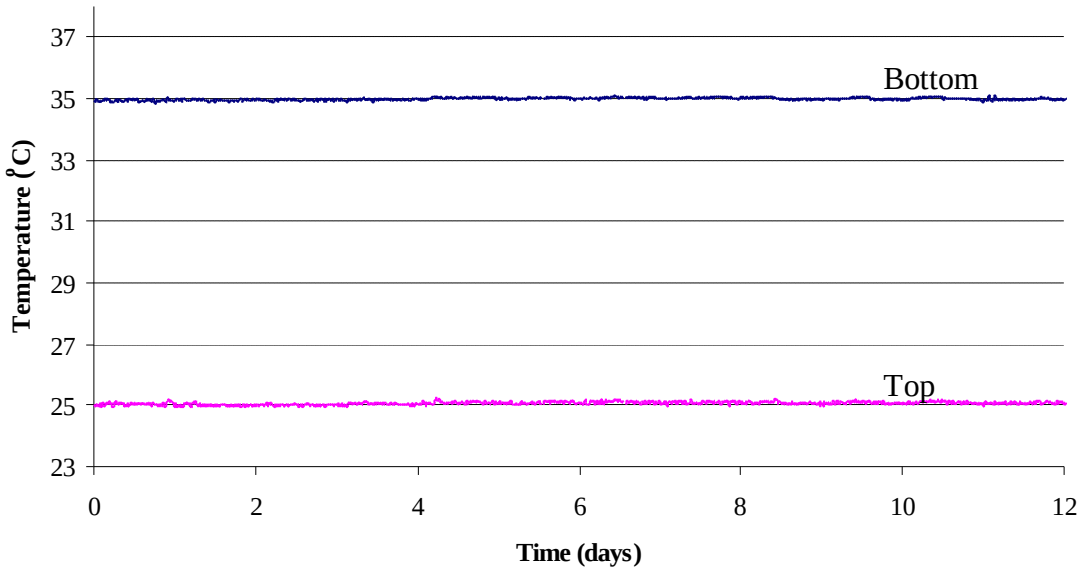

Figure 3.1 Temperature control typical plot.

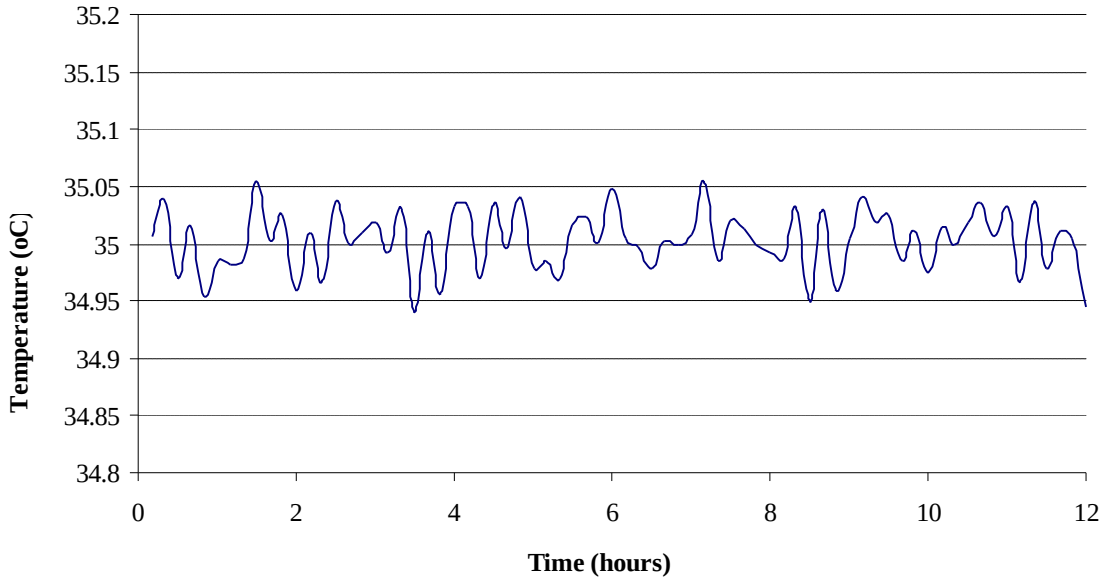

Figure 3.2a Temperature variation, typical plot for bottom chamber.

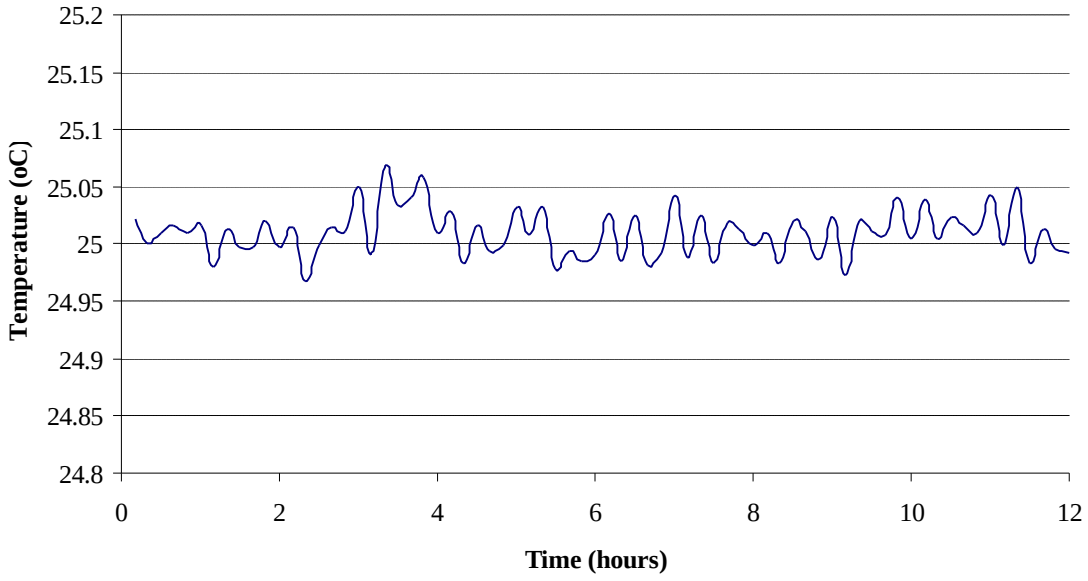

Figure 3.2b Temperature variation, typical plot for top chamber.

3.1.3 Relative Humidity Control

Control of the relative humidity is essential to the adequate performance of the apparatus and the validity of results. As explained earlier, the relative humidity range of the apparatus depends on the temperature of the surroundings. For this reason, prior to every experimental run the dew-point temperature is calculated to ensure that no condensation occurs within the system. During the experimental procedure, the apparatus was run under conditions ranging from 22.8 to 52 per cent relative humidity. Figure 3.3 corresponds to the relative humidity conditions for Test 10.

Figure 3.4 is a large-scale version of data shown in Fig. 3.3. It is clear from this plot that the maximum variation of the relative humidity control system is within ±0.1 of a percentage point from the set point.

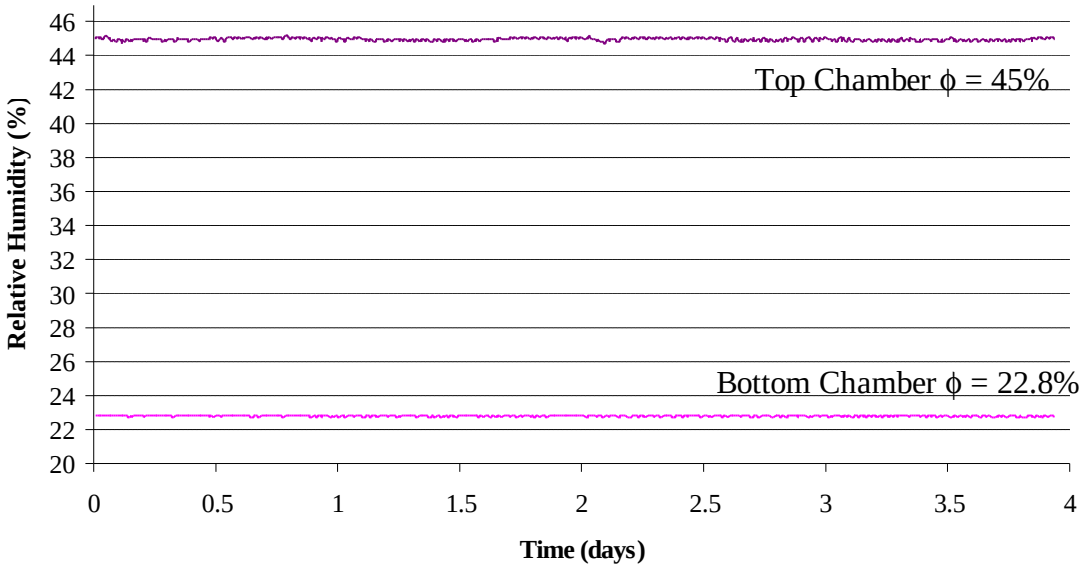

Figure 3.3 Relative humidity plot for Test No.10.

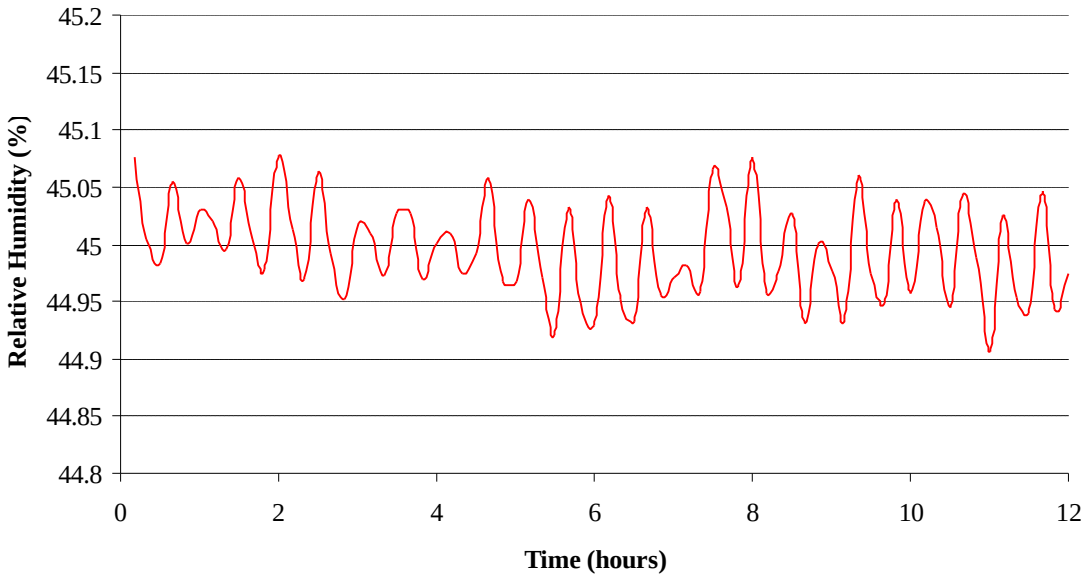

Figure 3.4 Relative humidity control for Test No. 10.

3.1.4 Pressure Control

As discussed in Chapter 2, the pressure control of the apparatus is essential to the moisture diffusion across the specimen. The pressure control system prevents the introduction of a pressure difference as an additional mechanism to the moisture diffusion. The pressure across the test material was controlled and maintained approximately equal by using rubber bladders as shown in Fig. 2.1. The pressure difference between the chambers was measured by a Datametrics micro-manometer, as described in Chapter 2. The pressure difference between the chambers and the atmosphere was measured with a U-tube mercury manometer.

Although rubber bladders were used to equalize the pressure between the chambers, a very small pressure difference was observed. Several attempts were made to cancel the small difference in pressure, but it was later concluded that the difference is inherent for the FDC and cup apparatuses. The pressure difference is further analyzed in the next section.

The control accuracy of the ASHRAE FDC allows the moisture transfer across the specimen to be measured, as a result only of the temperature and humidity gradients. The results obtained from the tests performed are discussed in the following section.

3.2 RESULTS

Two different sets of experiments were conducted in order to validate the operation of the experimental apparatus. The first set of experiments (*Moisture Permeance*) measured the moisture transfer through the specimen under both isothermal and nonisothermal conditions. The second experimental set (*Air Permeance*) allows for the calculation of the air permeance of the specimen. This last experimental set was conducted as a result of findings encountered during the first experimental set.

The purpose of moisture permeance measurements is to validate the diffusion model. Conditions were set according to the various existing models. As discussed

previously, a necessary condition for the validation of the model is that moisture transfer must cease when the diffusion potential is the same on both sides of the specimen. The models based on the gradient of chemical potential, moisture concentrations, activated moisture molecules, and vapor pressure were tested.

A standard ASTM cup method test is included in this experimental set. As stated in Chapter 1, the cup test is an experimental method used to determine the moisture permeance for a given material under isothermal conditions.

3.2.1 Moisture Permeance

The purpose of this experimental set includes investigating various moisture diffusion models, as well as validating the apparatus. This experimental set includes a series of isothermal and nonisothermal measurements conducted with the ASHRAE FDC, and a set of experiments based upon the ASTM standard cup test.

Isothermal Tests

Two isothermal tests were conducted in order to obtain information regarding the specimen and verify the operation of the control systems. The data obtained during these tests were used to calculate the permeance of the specimen. The data collected and permeance results as shown in Tables 3.1 and 3.4, respectively, are used in later sections for comparison and validation purposes. The calculation of the moisture transfer follows the procedure outlined in Sections 2.5 and 2.6.

Table 3.1 Isothermal experimental results and conditions.

Case	n" x10^8 **(kg/m^{2}s)**	Uncertainty x10^8 **(kg/m^{2}s)**	ϕ_t (%)	$\mathbf{T_t}$ (C)	ϕ_b (%)	$\mathbf{T_b}$ (C)
Isothermal No. 1	3.505	0.221	58	24	43	24
Isothermal No. 2	3.136	0.196	23	25	33	25

Nonisothermal Test

Current diffusion models were tested under nonisothermal conditions. A total of five diffusion models based upon the gradient of chemical potential, moisture concentration, water vapor concentration, vapor pressure and activated moisture molecules were tested. As explained previously, a necessary condition for the validation of the potential diffusion model is that the moisture diffusion must cease when the transfer potential or driving force is equal on both sides of the specimen. In order for the gradient of the potential to be zero, conditions were calculated such that, the potential given by each candidate model would be the same on both sides of the specimen. The calculation procedure for the values corresponding to the potential for each one of the models in each chamber is shown in Appendix A; the results are shown in Table 3.2.

Table 3.2 summarizes the results obtained from the diffusion potential tests. This table shows the measured moisture flux rate across the specimen, the vapor pressure and the conditions corresponding to each chamber for the respective model. Figure 3.5 shows the results obtained from moisture diffusion tests. The models were tested while maintaining the conditions of the top chamber constant at 25°C and 45 per cent relative humidity. Among the models tested, the vapor pressure (P_v) and the water-vapor concentration (P_v/T) models best satisfied the null flow condition. Although the water-vapor concentration and the vapor pressure model yield similar results, the vapor pressure model best satisfied the null-flow condition needed for the validation of the diffusion model.

Figure 3.6 shows the results obtained from moisture diffusion tests as a function of the vapor pressure for the bottom chamber. This figure depicts the moisture flux for each model while maintaining the corresponding potential equal to zero. A straight line was traced along the results obtained from each model. The constant slope of this line shows the permeance (g) to be constant under the range tested, where the permeance is given by,

$$g = \frac{\Delta P_v}{\dot{n}''} \tag{3.1}$$

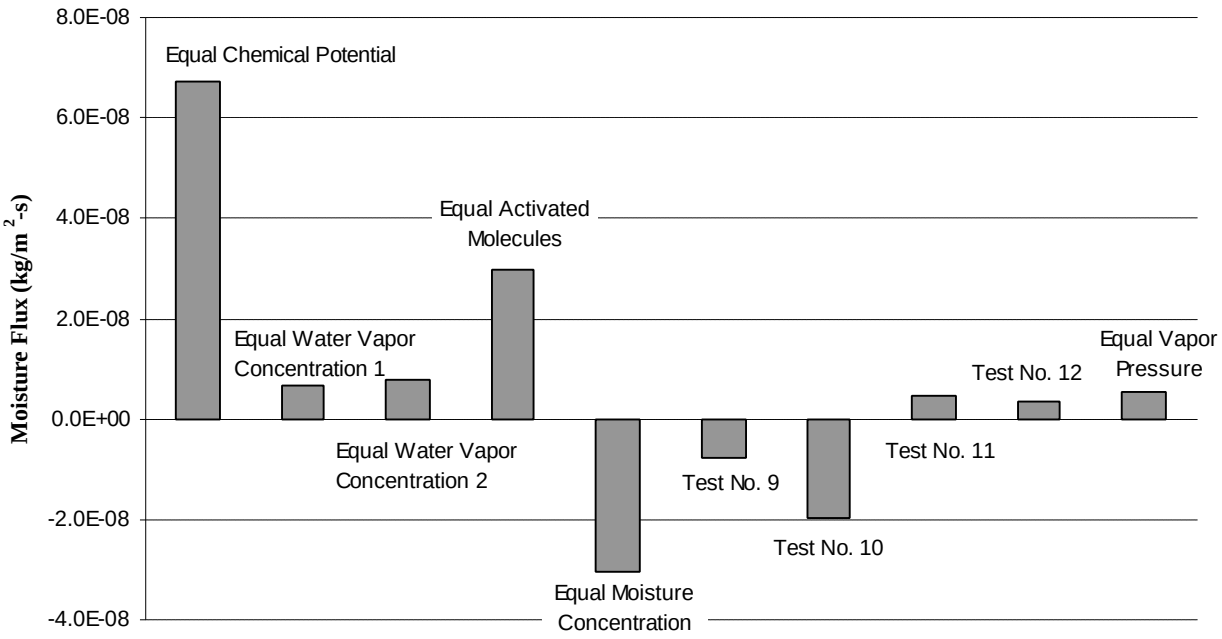

Figure 3.5 Evaluation of moisture diffusion theories.

Although some uncertainties in the calculation of the conditions for the activated moisture model were considered, the results obtained for this case were significantly poorer for the null condition compared to the vapor pressure model. The sorption isotherm (Burch,1993) and the activated energy formulation for the OSB (Siau) are among these uncertainties.

Additional ASHRAE FDC Tests

Most of the experimental cases were conducted near room temperature with a temperature difference of either 5°C or 10°C across the specimen. However, in order to verify the results previously obtained from the vapor pressure model, a low temperature test (Test No. 12) was conducted. The results of this test are shown in Fig. 3.6. Each symbol (with estimated uncertainty bands) in Figures 3.5 and 3.6 represents the average of a series of runs (4-10) of each experimental case.

Table 3.2 Nonisothermal experimental results and conditions.

Case	n" x10^8 (kg/m^2-s)	Uncertainty x10^8 (kg/m^2-s)	f_t (%)	T_t (C)	f_b (%)	T_b (C)	P_{vb} (kPa)	P_{vt} (kPa)
Equal Chemical Potential	6.741	0.714	45	25	52	30	2.226	1.425
Equal Moisture Concentration	-3.036	-0.303	45	25	45	20	1.052	1.425
$(Pv/T)_t=(Pv/T)_b$ Tb-Tt = 5C	0.623	0.195	45	25	34.1	30	1.443	1.425
Equal Vapor Pressure Tb-Tt = 10C	0.554	0.190	45	25	25.3	35	1.425	1.425
$(Pv/T)_t=(Pv/T)_b$ Tb-Tt = 10C	0.790	0.315	45	25	26.1	35	1.467	1.425
Equal Activated Moisture	2.968	0.391	45	25	31.9	30	1.793	1.425
Test No. 9	-0.771	0.200	45	25	22.8	35	1.283	1.425
Test No. 10	-1.951	0.445	22.8	35	45	25	1.283	1.282
Test No. 11	-0.476	0.421	25.3	35	45	25	1.425	1.423
Test No. 12	0.330	0.0524	45	5	32	10	0.392	0.392

Note : Positive moisture flux denotes transfer from the bottom chamber to the top.

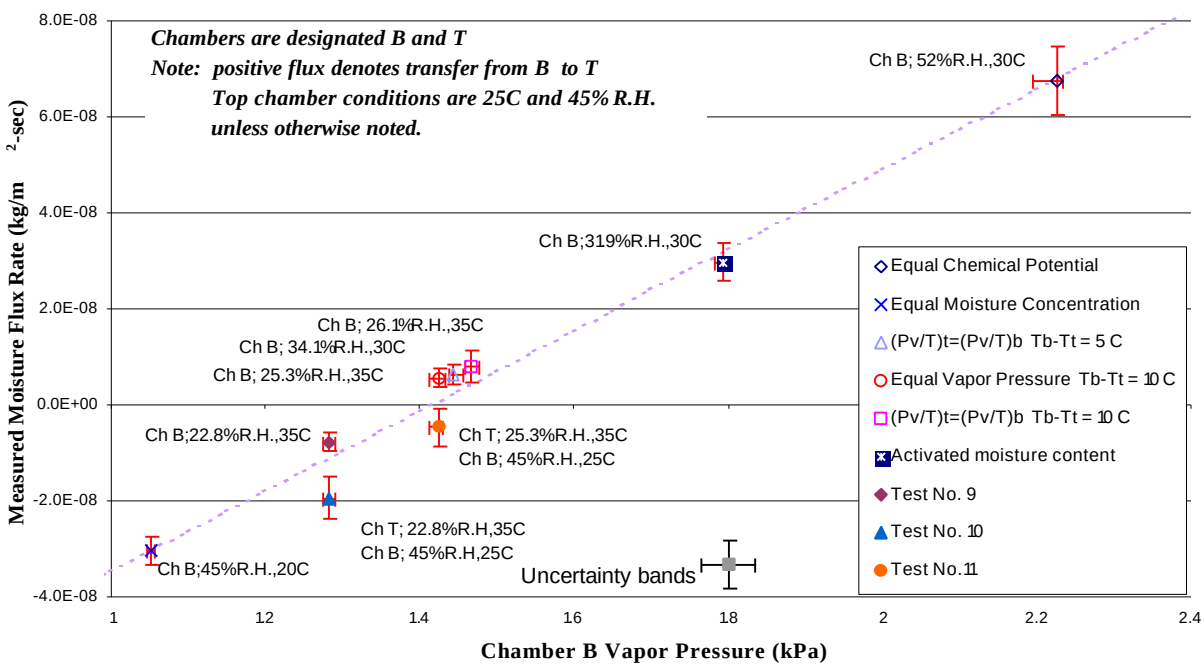

Figure 3.6 Moisture diffusion theories vs. vapor pressure difference.

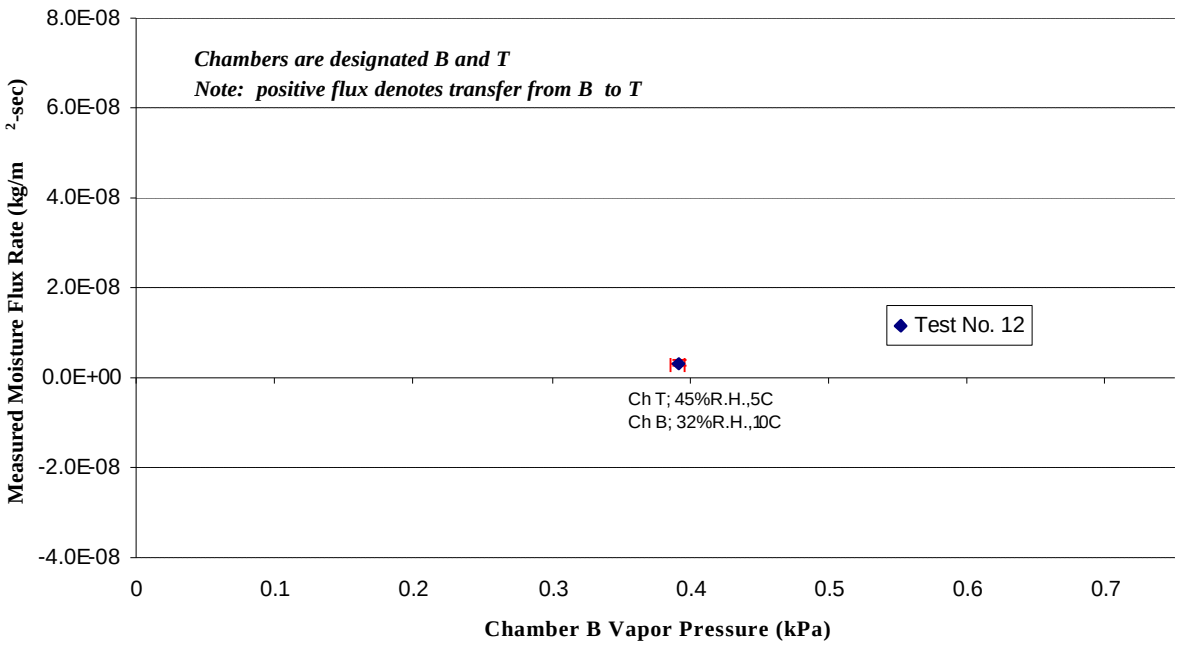

Figure 3.7 Evaluation of the vapor pressure diffusion model at low temperatures.

A series of additional tests were conducted to determine the moisture diffusion behavior near the equal vapor-pressure point. Tests denoted as Test No. 9 and Test No. 10, were conducted to confirm the reversal of the moisture flow near the equal-vapor pressure condition. Test No. 11 was conducted to observe the effect of buoyancy (gravity) in moisture diffusion.

The flow reversal test was performed by selecting the conditions of the lower chamber for which a change in the flow direction would be expected. As depicted in Fig. 3.5, the flow direction was changed when the vapor pressure gradient was reversed.

Moiser (1996) reported that the effect of gravity in the moisture diffusion mechanism is negligible. The results of Test No. 11 suggest a small buoyancy effect. This test was performed by interchanging the conditions of the chambers and observing the direction of the moisture flow in contrasts to the original chamber state. For a given set of conditions for the top and bottom chamber, the moisture flow direction is considered to be positive if moisture is being transfer from the bottom chamber to the top. The results for the vapor pressure model test showed a very small positive flow of

moisture. When the chamber conditions were interchanged in Test No. 11, the flow was of the same order of magnitude but in the opposite direction. This last observation supports the statement by Moiser. The complete set of data attained for each of the experimental models is displayed in Appendix B.

ASTM Standard Cup Test

The cup experiments were based upon the ASTM test method 96-80 (ASTM 1989), and the research conducted by Burch and Thomas in 1992. This experimental method was used to determine the permeance of the OSB specimen by measuring the water-vapor transmission through the specimen. The complete experimental procedure of these tests has been discussed in Chapter 1.

A total of three-cup measurements were made for the test material. Measurements made of the moisture transfer (*WVT*) in each cup allowed for the calculation of the permeability (m, or permeance g as a function of the average relative humidity across the specimen. The measurements were conducted at a constant temperature of approximately 25°C. The results obtained are shown in Table 3.3.

Table 3.3 Cup test experimental results.

	Cup I	**Cup II**	**Cup IV**
Mean R.H.	16.98	38	79.92
R.H. Difference	11.37	10.31	9.18
WVT x10^{10} **(kg/s)**	3.839	3.142	5.486
gx10^{11}**(kg/m-sec-Pa)**	9.19	8.28	16.60

The relative humidity difference denotes the difference across the specimen generated by aqueous salt solutions, as shown in Table 1.1. The complete experimental data and results are shown in Appendix A.

3.2.2 Validation of Data

The validation of the data is accomplished by comparing the results obtained from ASHRAE FDC and previously published results for the same material.

The permeance of the test material was determined by using the moisture transfer data obtained during both isothermal and nonisothermal tests. As discussed in Chapter 1, the permeability (permeance) data obtained from isothermal tests are applicable to nonisothermal tests as well, (Galbraith and McLean, 1998). The reduced permeance data can be then validated by comparing it to published data of the same type. In this case the permeance information from the tests were compared to data obtained by the National Institute of Standards and Technology (NIST) (Burch and Thomas, 1992). Table 3.4 shows the data in its reduced form.

Figure 3.7 shows the reduced data for the various tests (isothermal, nonisothermal and ASTM cup tests) as indicated in Table 3.4 and the data reported by NIST, for OSB at 24°C. Permeance data is not available either at lower or higher relative humidity as a result of the apparatus limitation by condensation. However, the ASHRAE FDC data agrees well with the data obtained from the conventional cup test and the published data. The dotted line in Fig. 3.7, indicates the linearity behavior of the permeance in the experimental range.

Table 3-4 Permeance results from ASHRAE FDC and cup tests.

Case	**Mean R.H.**	g x10^{11} **(kg/m^2-s-Pa)**
Isothermal Test No. 1	50.0	7.84
Isothermal Test No. 2	28.0	9.47
Test No. 1	38.4	8.06
Test No. 2	45.0	8.14
Test No. 3	48.5	8.42
Cup 1	16.9	9.19
Cup 2	38.0	8.28
Cup 4	79.9	16.60

The permeance was determined by using a modified form of Fick's law given by Eq. 1.2.

$$g = \frac{\dot{n}''}{\Delta P_v} \tag{3.1}$$

where $\dot{n}''$ is the flux of moisture and DP_v is the difference in vapor pressure. As the moisture flux approaches zero, the corresponding permeance is undefined. For this reason the permeance corresponding to the vapor pressure and the water-vapor concentration models test cannot be determined.

Table 3.4 summarizes the results of the permeance data obtained from both the ASHRAE FDC tests and the ASTM standard cup tests. The temperature and relative humidity conditions corresponding to isothermal tests are shown in Table 3.1. The conditions of the tests labeled in Table 3.4, as Test No.1, 2, and 3, correspond to the conditions of those shown in Table 3.2 for the activated moisture, moisture concentration and chemical potential models, respectively.

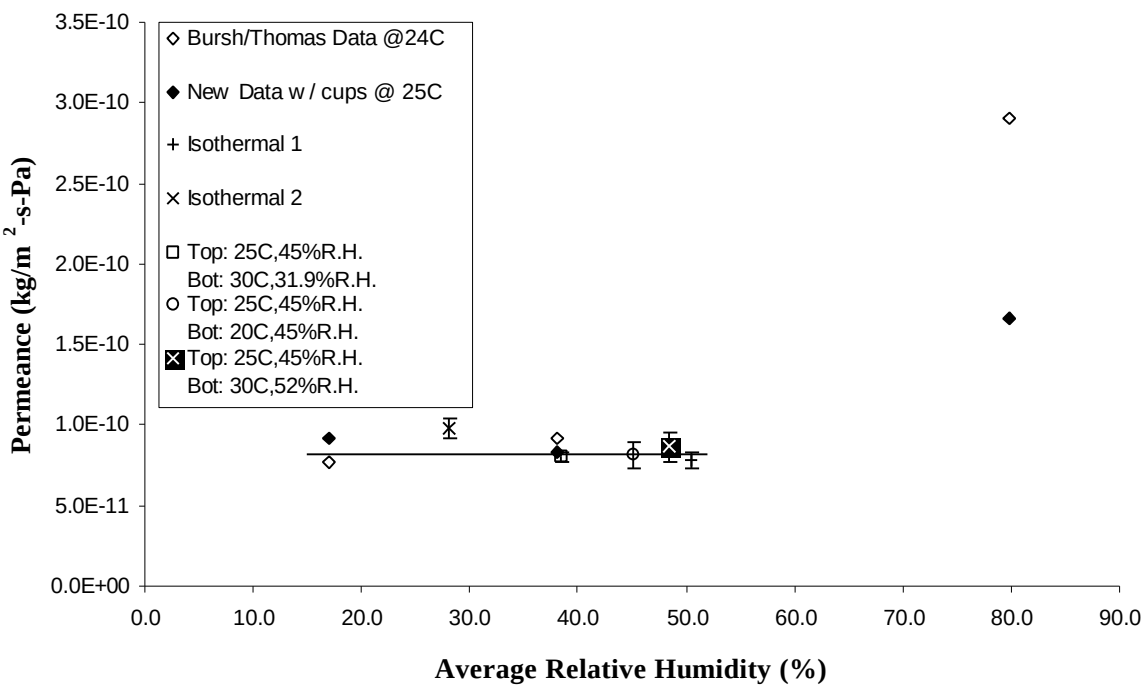

Figure 3.8 Comparison of permeance data from the ASHRAE and cup apparatuses.

Unexpected Findings

During the ASHRAE FDC experimental procedure, a small difference in the static pressure between the chambers was found. This pressure difference was first detected by a Magnehelic™ pressure differential gauge with a resolution of ±0.02 iwg. The pressure difference was attributed originally to leakage in the system. However, the difference was still observed after extensive leak-control measures were implemented. The static pressure was observed to be always higher in the chamber where moisture was being transferred.

An experiment was designed to determine if the difference in static pressure across the specimen is attributed to the diffusion of moisture. The test utilized the experimental setup of the ASTM standard cup test and a digital micro-manometer transducer. Figure 3.8 shows the schematic of the experimental setup. A small adapter was designed to fit the ASTM cup. This adapter enables a digital Datametrics micro-manometer as described in Chapter 2, to read the static pressure difference across the specimen between the cup and vessel. The specimen was perforated by a small stainless steel tube, which was connected to the instrument at the top of the vessel by a small diameter plastic tube. The instrument at the top of the vessel was connected to the digital micro-manometer, where the pressure difference was measured.

The experimental results showed a static pressure difference of 0.0032 iwg across the specimen and opposing the moisture flow direction. The pressure difference and the moisture transfer were periodically measured for a period of several weeks.

The pressure difference across the specimen is believed to be caused by bulk airflow generated by the process of air diffusion. The bulk flow of air governed by Darcy's equation balances the diffusion of air in the opposite direction as a result of the gradient in the partial pressure of (dry) air.

Additional attempts to use the digital micro-manometer to measure this difference failed in other cups and over extended times. The reason is that the micro manometer cannot tolerate the corrosive effects of the salts in the sealed environment.

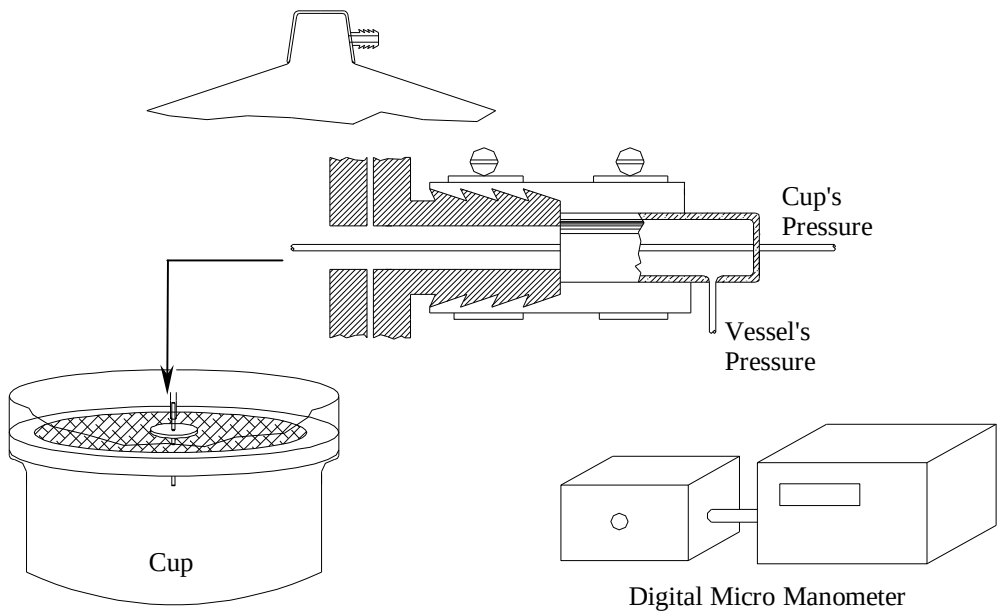

Figure 3.9 Static pressure difference experimental setup.

3.2.3 Air Permeance

An experiment to measure the bulk flow as a result of the difference in static pressure found across the sample was designed. The flow of air is given by Darcy's Equation as

$$\dot{n}_a = m_a A_s \frac{\Delta P_s}{\Delta L} \tag{3.2}$$

where m_a is the air permeability, A_s is the cross-sectional area of the material, DP_s is the static pressure difference, and DL is the thickness of the material.

The air permeance of the material was determined by measuring the pressure drops across the OSB specimen over a range of air flow rates. A schematic of the experimental setup is shown in Fig. 3.9.

The airflow to the chamber was supplied by a dry-air generator and regulated by a needle valve in the flowmeter. The pressure was measured at various air flow rates, hence, permitting the calculation of the air permeability by manipulating Eq. 3.2

$$m_a = \frac{\dot{n}}{\Delta P_s}\frac{\Delta L}{A_s} = \frac{\Delta L}{mA_s} \tag{3.3}$$

where, m denotes the slope of the plot in Fig. 3.10. Figure 3.10 shows the data and the calculated air permeability (m_a). A small discrepancy was found between the measurements made by the two flowmeters, as a result of their accuracy. However, the slopes corresponding to both flowmeters differed only one per cent. The air permeability of the material was determined by using the average of the slopes for each of the flowmeters. The air permeability for OSB was calculated to be 1.322×10^{-8} kg/Pa-s-m.

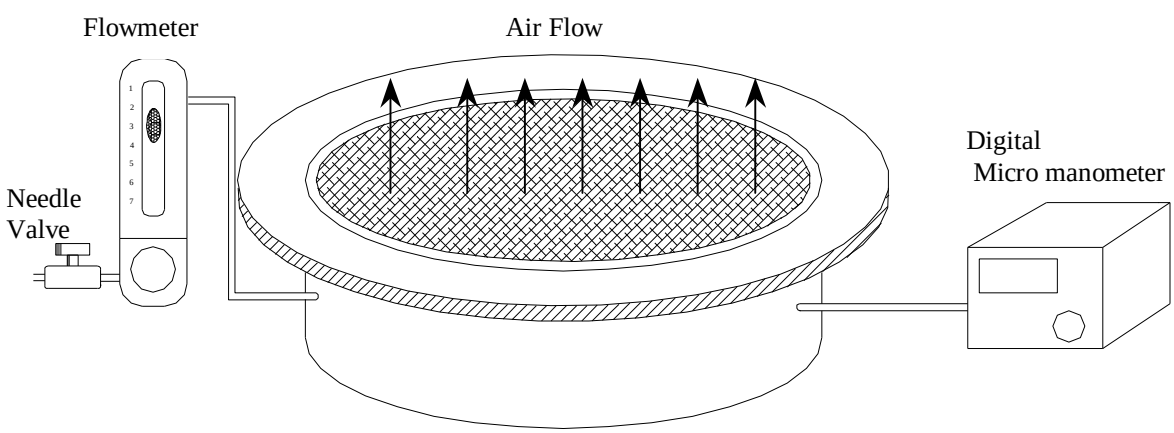

Figure 3.10 Air permeance experimental setup.

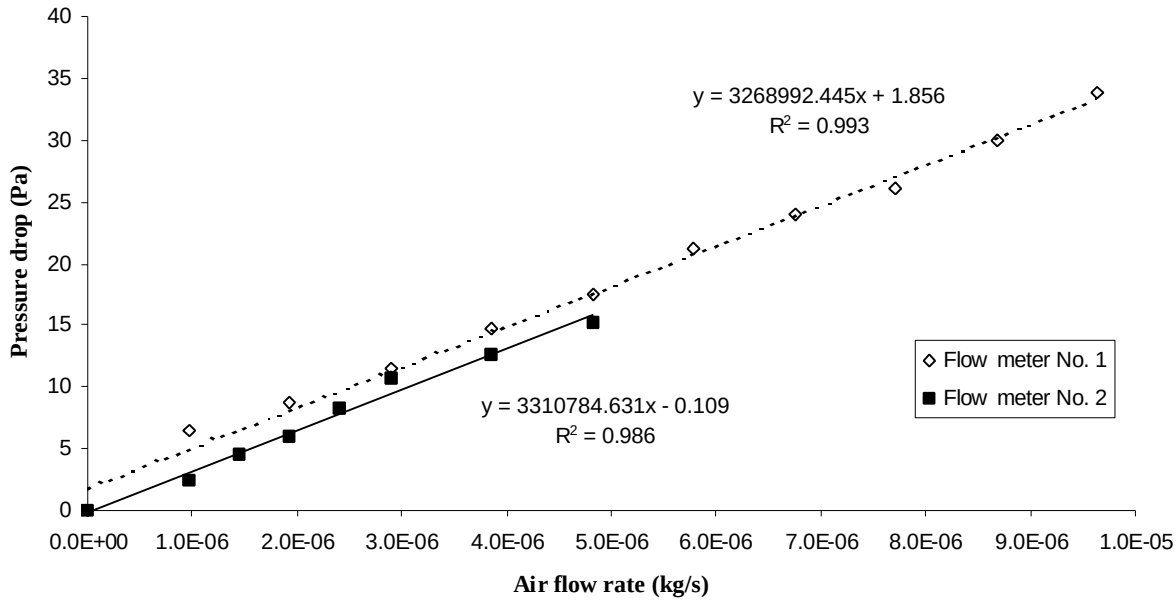

Figure 3.11 Air permeability data and results. (1 lb/h = 1.26E-04 kg/s), (1 iwg = 249 Pa)

The results show that bulk airflow of approximately 1.890E-6 kg/s (0.015 lb/h) occurs through the specimen of OSB for the pressure difference of 0.7968 Pa (0.0032 iwg) measured in the ASTM cup test. Further investigation of this coupled effect on bulk flow by diffusion of water vapor and (dry) air is beyond the scope of the present research.

3.3 SUMMARY

The objectives of the research included the validation of the existing apparatus operation and the study of the various moisture diffusion models. These two objectives have been accomplished. The permeance results obtained from the ASHRAE FDC and the ASTM cup tests agreed well with the data reported by the NIST. The satisfactory operation of the ASHRAE FDC is validated by the agreement between the measured and published results.

The theory that moisture diffusion under nonisothermal conditions is governed by the gradient of the water-vapor pressure is strongly supported by the results obtained

from the ASHRAE FDC method. The results obtained from the tests of the vapor pressure model conducted near room temperature, and low temperature, were of good agreement with the null-flow condition. None of the other proposed models approached the null-flow necessary condition nearly as well.

Further investigation of the significance of difference in static pressure across the OSB sample while experiencing moisture diffusion is recommended.